Vector Fluxgate Magnetometer (VMAG) Development for DSX

Mark B. Moldwin

UCLA
Institute of Geophysics and Planetary Physics
Department of Earth and Space Sciences
3845 Slichter Hall
Los Angeles, CA 90095-1567

Final Report

03 June 2010

AIR FORCE RESEARCH LABORATORY
AIR FORCE MATERIEL COMMAND
Space Vehicles Directorate
29 Randolph Rd.
Hanscom AFB, MA 01731-3010

AFRL-RV-HA-TR-2010-1056

This technical report has been reviewed and is approved for publication.

/ signed / / signed /

Arthur J. Jackson   Dwight T. Decker, Chief
Contract Manager   Space Weather Center of Excellence

REPORT DOCUMENTATION PAGE

Form Approved
OMB No. 0704-0188

Public reporting burden for this collection of information is estimated to average 1 hour per response, including the time for reviewing instructions, searching existing data sources, gathering and maintaining the data needed, and completing and reviewing this collection of information. Send comments regarding this burden estimate or any other aspect of this collection of information, including suggestions for reducing this burden to Department of Defense, Washington Headquarters Services, Directorate for Information Operations and Reports (0704-0188), 1215 Jefferson Davis Highway, Suite 1204, Arlington, VA 22202-4302. Respondents should be aware that notwithstanding any other provision of law, no person shall be subject to any penalty for failing to comply with a collection of information if it does not display a currently valid OMB control number. **PLEASE DO NOT RETURN YOUR FORM TO THE ABOVE ADDRESS.**

1. REPORT DATE *(DD-MM-YYYY)*	2. REPORT TYPE	3. DATES COVERED *(From - To)*
03-06-2010	Annual Report	April 2009 – April 2010

4. TITLE AND SUBTITLE	5a. CONTRACT NUMBER
	FA8718-05-C-0025

Vector Fluxgate Magnetometer (VMAG) Development for DSX

5b. GRANT NUMBER

5c. PROGRAM ELEMENT NUMBER
62601F

6. AUTHOR(S)
Mark B. Moldwin

5d. PROJECT NUMBER
1010

5e. TASK NUMBER
RR

5f. WORK UNIT NUMBER
A1

7. PERFORMING ORGANIZATION NAME(S) AND ADDRESS(ES)
UCLA
Institute of Geophysics and Planetary Physics
Department of Earth and Space Sciences
3845 Slichter Hall
Los Angeles CA 90095-1567

8. PERFORMING ORGANIZATION REPORT NUMBE

9. SPONSORING / MONITORING AGENCY NAME(S) AND ADDRESS(ES)

Air Force Research Laboratory
29 Randolph Road
Hanscom AFB, MA 01731-3010

10. SPONSOR/MONITOR'S ACRONYM(S)

AFRL/RVBXR

11. SPONSOR/MONITOR'S REPORT NUMBER(S)
AFRL-RV-HA-TR-2010-1056

12. DISTRIBUTION / AVAILABILITY STATEMENT

Approved for Public Release; Distribution Unlimited.

13. SUPPLEMENTARY NOTES

14. ABSTRACT
UCLA built and delivered a three-axis fluxgate magnetometer for the AFRL-mission. The instrument is designed to measure the medium-Earth orbit geomagnetic field with precision of 0.1 nT and provide the field direction to within 1 degree. The instrument will provide the DC magnetic field for phase space density calculations of energetic particles, the magnetic field vector information for the Loss Cone Imager (LCI) payload, and the ULF wave environment. The project delivered the flight unit in November 2008. Integration and Testing of VMAG and pre-launch testing and on-orbit calibration remain.

15. SUBJECT TERMS
Space Instrumentation, magnetometer, radiation belts

16. SECURITY CLASSIFICATION OF:			17. LIMITATION OF ABSTRACT	18. NUMBER OF PAGES	19a. NAME OF RESPONSIBLE PERSON
					Daniel L. Elsner, 1st Lt
a. REPORT	**b. ABSTRACT**	**c. THIS PAGE**	SAR	19	19b. TELEPHONE NUMBER *(include area code)*
U	U	U			

Standard Form 298 (Rev. 8-98)
Prescribed by ANSI Std. Z39.18

(Blank Page)

Contents

Figures

Tables

1. INTRODUCTION

This effort was in response to the Battlespace Environment Division, Space Vehicle Directorate, Air Force Research Laboratory's (AFRL) request to develop and provide a vector fluxgate magnetometer to support both the Space Weather (SWx) and Wave Particle Interaction (WPIx) payloads on the Demonstration and Science Experiment (DSX), which will be launched into the Medium-Earth Orbit Space Environment Regime.

Included as part of the DSX payload is a vector magnetometer. The vector magnetometer provides measurements of the terrestrial field, which is essential to fulfill the two primary goals of the DSX science program. The fluxgate magnetometer provides the necessary data to support both the SWx specification and mapping requirements and the WPIx requirements. The magnetic field is necessary to reconstruct pitch-angle distributions (PADs), to calculate phase space densities, and to determine important local plasma parameters such as plasma beta and the local index of refraction. The fluxgate magnetometer provides measurements of the magnetic fields caused by currents that flow into and above the Earth's ionosphere. These currents close with currents in the Earth's magnetosphere, via field-aligned currents, and measuring these currents is essential for improvements in magnetospheric specification models.

This Report gives an overview of the science rationale and objectives, a description of the heritage of the instrument, the design of the magnetometer, and briefly summarizes our activities, accomplishments, and lessons learned during this year (April 2009 – April 2010). The reader is referred to the Year 1, 2, 3 and 4 Annual Reports (AFRL-VS-HA-TR-2006-1079, AFRL-RV-HA-TR-2007-1077, AFRL-RV-HA-TR-2008-1108, AFRL-XX-YY-2009-XYZZ) for the initial development of the engineering unit. Other information regarding the VMAG instrument is found in the Preliminary Design Review and Critical Design Review documentation submitted to the DSX Project Management Office (PMO) as part of the regular reporting process. We have developed a magnetometer that easily conforms to the DSX requirements (as specified in L0/L1 Requirements Document and Common Requirements Document Rev D), with a high degree of reliability and a low impact on spacecraft resources in terms of mass, power, and volume.

2. BACKGROUND

This section provides the Science Rationale, the Magnetometer Heritage, the Magnetometer Design and a listing of the VMAG team. The subsequent section present a summary of the activities conducted for this project this past year (April 2009 – April 2010).

2.1. Science Rationale

As an educational institution, UCLA's primary motivation in providing fluxgate magnetometers for DSX is directed to the scientific return from the mission. Improving our scientific understanding often goes hand-in-hand with improving the technology of our scientific instrumentation. Hence, UCLA's strong interest over the years in continuing to develop science-grade magnetometers. The DSX mission clearly benefits

from this extensive heritage in scientific instrumentation. Moreover, UCLA's effort will contribute to the operational goals of DSX, which allows UCLA to provide an immediate societal benefit. This return of investment for the nation is also important for UCLA, allowing us to show the value in conducting basic research.

The magnetometer is essential for fully characterizing the particle and wave data to meet the Space Weather and WPIx goals. However, in addition to the supporting role of the magnetometer, the data provided by the instrument will clearly be a valuable resource for the Space Physics Community on its own. At UCLA, our scientific efforts are centered around the observations of magnetic fields due to current systems in the Earth's ionosphere and magnetosphere and to the ULF wave environment. There have been very few spacecraft with research-quality vector magnetometers flown in MEO. Therefore, the DSX mission will be ground-breaking in terms of providing information about the Earth's geomagnetic field and ULF wave environment in the inner magnetosphere.

The MEO magnetospheric regime has not been extensively studied because most scientific satellites are either in LEO-Low Earth Orbit (e.g., SAMPEX), HEO-highly elliptical orbit (e.g., SCATHA, AMPTE, ISEE 1/2), or at GEO-Geosynchronous orbit (e.g., GEOS 2, the LANL spacecraft). MEO covers a range of interesting space physics regimes including the radiation belts, the ring current, and the plasmasphere, and is home to a growing number of satellites (such as GPS) thus understanding the MEO space weather environment is becoming more and more important [e.g., *Le and Russell,* 1993].

2.2. The DSX Mission VMAG Science Objectives

The specific region of the magnetosphere to be explored by the DSX satellite between 10,000- and 20,000-km altitude (*L* between 1.5 to 3.1) is now known to be an extremely dynamic region overlapping the radiation belt slot, a region where the plasmapause often resides, and a place of intense wave activity [e.g., *Baker et al.,* 1994, *Moldwin et al.,* 2002, *Bortnik et al.,* 2003, *O'Brien et al.,* 2003]. The location of the inner edge of the outer radiation belts and the plasmapause has been found to be highly correlated [e.g., *Li et al.,* 2006]. Figure 1 shows this correlation using data from SAMPEX and the O'Brien and Moldwin model for the location of the plasmapause. This correlation suggests that the plasmasphere plays a role in the loss of the energetic electrons. However, in addition, it has been shown in a model that radiation belt electrons of energies of > 1 MeV can be energized by ring current ion driven ULF waves just outside the plasmapause [*Ozeke and Mann*, 2008]. The DSX mission will be able to directly test these results.

In addition, DSX will provide the study of ring current dynamics and field-aligned currents (FAC) from a unique perspective deep in the inner magnetosphere. Two specific questions to be addressed by DSX are (1) what is the ULF wave environment in the inner magnetosphere during severe geomagnetic storms and (2) what is the configuration of the inner magnetospheric magnetic field during storms? With one satellite, it is difficult to place the observations into global context – however, UCLA operates three mid-latitude magnetometer chains (MEASURE, SAMBA, and McMac) that span the DSX *L* shells and can be used to estimate the inner magnetospheric mass density, independently estimate the location of the plasmapause, and characterize the global ULF wave environment. The PI for this proposal is the PI for MEASURE and a co-PI for SAMBA and McMac.
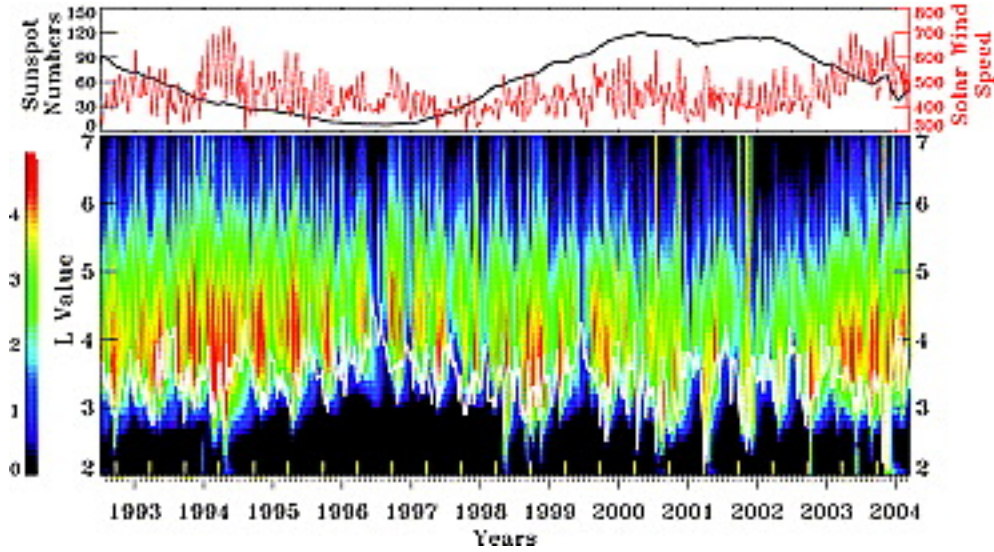
Figure 1. (top) Variations of yearly window-averaged sunspot numbers (black curve) and weekly window-averaged solar wind speed (km/s, red curve). (bottom) Monthly window-averaged, color-coded in logarithm, and sorted in L (L bin: 0.1) electron fluxes of 2–6 MeV (#/cm2-s-sr) by SAMPEX since its launch (July 3, 1992) into a low-altitude (550 × 600 km) and highly inclined (82°) orbit. The superimposed white curve represents every 10-day's minimum Lpp based on an empirical model [*O'Brien and Moldwin*, 2003]. The yellow vertical bars on the horizontal axis are marks of equinoxes.

These complementary ground-based datasets will be used in addressing both questions. Specifically, for question (1), we will compile a database of ULF wave power as a function of LT, Magnetic latitude, *L* shell, and geomagnetic activity (as indicated by Dst, Asym, SymH, Kp, and AE) by automatically calculating dynamic power spectra. The result will be similar to the survey of AMPTE data by *Anderson et al.* [1990], but will cover the inner magnetospheric region.

For question (2), a satellite in a 10,000 x 20,000 elliptical orbit would have an orbital period of about 3 hours and 20 minutes. This is comparable to the time scale of the main phase of a geomagnetic storm. Therefore, DSX will sample a range of local times during the main phase of each storm allowing for the examination of the evolution of the partial ring current for a variety of storms. Recent studies have shown that the inner magnetosphere can be severely distorted during geomagnetic storms due to the growth of the partial ring current [e.g., *Tsyganenko et al.*, 2003].

2.3 MAGNETOMETER HERITAGE

The UCLA fluxgate magnetometer has been employed in state-of-the-art investigations of magnetospheric and solar system magnetic fields for over 35 years. During this time the accuracy and precision of the magnetometer has grown even as its mass, size and power decreased. In this section we review the heritage upon which the UCLA ST5 design rests.

2.3.1 The Early Years: ATS, OGO 5, Apollo and PVO

UCLA has a long history of supplying science-grade magnetometers, as shown in Figure 2. The UCLA magnetometry group was established in the mid 1960s by P. J. Coleman when it furnished fluxgate magnetometers for ATS 1 and 6, and OGO 5. The ATS 1 instrument was a simple, spinning, two-axis instrument, very much in the spirit of "better, faster, cheaper" and innovative for its time. ATS 6 was a three-axis, inertially stabilized measurement. The OGO 5 magnetometer was the first magnetometer capable of accurately measuring both the full Earth's field and the smallest (interplanetary) magnetic fields in the neighborhood of Earth. It accomplished this with a ladder-adder network, basically a high-resolution A/D converter in which the basic magnetometer was embedded. While it was successful in many respects, it was very complex and calibration was time consuming. In 1971 and 1972 the Apollo 15 and 16 sub-satellites carried UCLA fluxgate magnetometers of a very simple design in a low field environment. In 1972 and 1973 UCLA was selected to build both the ISEE 1 and 2 fluxgate magnetometers as well as the Pioneer Venus orbiter magnetometer. Both presented challenging design issues but quite different ones. The ISEE magnetometer required a very precise measurement of a magnetic field whose strength varied from 5 nT to over 8000 nT. UCLA built a highly linear magnetometer with two gain states with a 12-bit A/D converter accurate to LSB. Oversampling and averaging provided 14-bit accuracy and 16-bit resolution. The richness of the scientific return from this instrument attests to the success of this approach. The Pioneer Venus spacecraft was a spinner whose data rate at times was insufficient to return even a vector-per-spin period. We developed a Walsh-Transform-based despinner to provide accurate vector information under all telemetry rates. The ISEE 1 and 2 spacecraft lasted 10 years and the Pioneer Venus mission lasted 14 years. The offsets and gain factors remained stable throughout the mission. All three magnetometers were still operating upon entry into the atmosphere.

2.3.2 Galileo

The innovation of the UCLA magnetometer group continued with development of the Galileo fluxgate magnetometer. This magnetometer with a 12-bit radiation hardened A/D converter with LSB accuracy again provided 16-bit resolution data through oversampling and averaging. In addition, it stored and returned despun average data between telemetry sessions so there could be total orbital coverage. This instrument launched in 1989 was still functioning normally after 14 years in space, much of which was in a very harsh radiation environment, when the spacecraft was intentionally plunged into Jupiter in September 2003.

UCLA / IGPP - Space Physics Magnetometer Projects

Years (columns): 65 | 66 | 67 | 68 | 69 | 70 | 71 | 72 | 73 | 74 | 75 | 76 | 77 | 78 | 79 | 80 | 81 | 82 | 83 | 84 | 85 | 86 | 87 | 88 | 89 | 90 | 91 | 92 | 93 | 94 | 95 | 96 | 97 | 98 | 99 | 00 | 01 | 02 | 03 | 04 | 05 | 06 | 07 | 08 | 09 | 10 | 11 | 12

Projects:
- ATS 1 Magnetometer
- Tungsten Magnetometer
- OGO 5 Magnetometer
- Apollo 15 Magnetometer
- Apollo 16 Magnetometer
- ATS 6 Magnetometer
- AFGL Mag Network
- ISEE 1 Magnetometer
- ISEE 2 Magnetometer
- PVO Magnetometer
- Galileo Magnetometer
- Mt St Helens Mag Network
- UK AMPTE Magnetometer
- POLAR Magnetometer
- FAST Fluxgate / Search Coil
- Brazil Magnetometer SACI-1
- Ground Magnetometers
- FedSat Magnetometer
- ST5
- Themis Ground
- DSX
- MMS

Figure 2. Spaceflight and ground-based magnetometer programs at UCLA over the last 35 years summarize the accomplishments of the group. Dark bars show fabrication and light bars show operational phases.

2.3.3 Polar

The Polar magnetometer launched in February 1996 is a highly accurate magnetometer with further advances in low noise and linearity. Polar has a 16-bit A/D converter and can amplify the signal by another factor of 8 so the basic magnetometer was designed to 19-bit precision in order to match its A/D accuracy. The magnetometer was accurate to within 0.01%. The success of this approach can be seen in the quality of the published results and the open access provided to all the data including the highest sampling rate data. These data can be accessed over the worldwide web at http://www-ssc.igpp.ucla.edu/forms/polar.

The Polar magnetometer included both an inboard and outboard magnetometer, each with two gain states to allow for measurements at perigee (2 Earth radii geocentric distance) and apogee (9 Earth radii). The Polar magnetometer was designed to sample data at 100 Hz, and with on-board averaging to obtain lower data rates. Two other magnetometers, that on FAST launched in August 1996, and that on FedSat launched in 2002, are simplified derivatives of the Polar design.

2.3.4 FAST

The FAST magnetometer, with a 64,000 nT range and 2 nT resolution, was designed to operate at low altitudes (< 4000 km altitude) with ambient fields ranging from 10,000 to 50,000 nT in magnitude. The FAST instrument could acquire data at a variety of rates,

up to 512 Hz. This instrument, which is still acquiring data after seven years of on orbit operations, formed the basis of the FedSat and ST5 designs. The FAST magnetometer demonstrated UCLA's ability to build highly reliable magnetometers with low noise levels, low non-linearities and stable (i.e., well behaved) offsets and gains for "full-field" operations.

2.3.5 FedSat

The FedSat magnetometer uses the highly successful Polar design with techniques to reduce mass and power developed on the FAST program and our ground-based effort. Figure 3 shows the FedSat engineering unit. The magnetometer has a 60,000 nT range and is sampled at either 10 or 100 Hz. The analog board weighs 200 g. A similar (analog only) instrument was fabricated and launched in September 1999 on the Brazilian SACI-1 micro-satellite but for unknown reasons no telemetry was received from the spacecraft despite a successful boost into orbit. Table 1 shows that mass of the basic UCLA magnetometer continued to shrink even as it grew more precise and accurate.
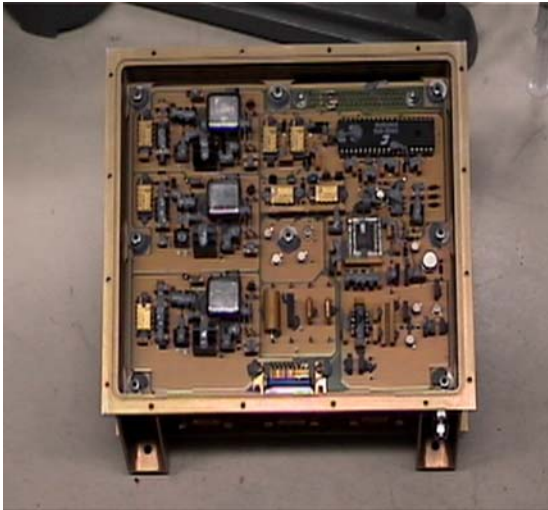
Figure 3. FedSat engineering unit showing electronics board and chassis.

Table 1. Modern Components and Continued Improvements Have Lowered the Mass of the UCLA Basic Circuitry.

Mission Name	Ranges [nT]	Cadence [Hz]	Mass [g]	Area [cm^2]
ISEE	8000, 556	4, 16	500	650
Galileo	16,000, 512, 32	0.05, 3, 32	500	650
Polar	47,000, 5700, 700	8.3, 100	400	450
FAST	64,000	Up to 512	350	400
FedSat	60,000	10,100	200	240

2.3.6 Ground-based Magnetometers

Deployment of UCLA's precision, low-cost, ground-based magnetometer for studying ionospheric and magnetospheric currents was a very important development in magnetometry at UCLA. This magnetometer can measure less than 0.1 nT in the full Earth's field with precision GPS timing control and costs less than $6000 to build. It is built on a PC board and installed in a PC chassis. The PC provides the power and accumulates the data. The circuit board is shown in Figure 4. UCLA has built and installed over 30 of these devices building ten at a time and testing them five at a time at its San Gabriel test site. These magnetometers are now operating from the Canadian arctic to the equator.

This effort enabled the UCLA team to become proficient in surface mount design and fabrication techniques. These techniques allowed the Polar design to be implemented on an 11 cm x 25 cm board, which is one quarter the board space originally used on Polar.
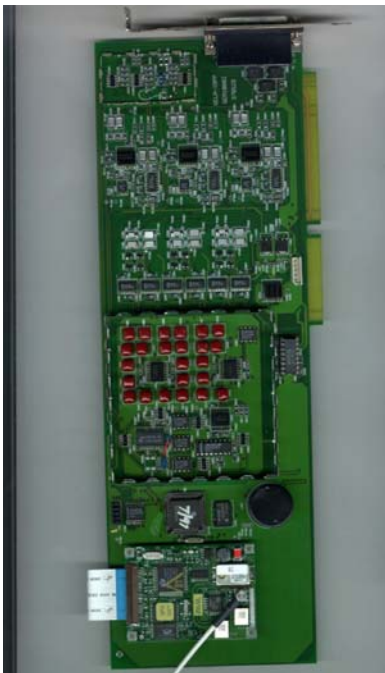
Figure 4. The circuit board of the ground-based magnetometer.

For the ST5 technology demonstration project, we used the same technology with an even simpler design to achieve a further reduction in board space.

2.4 MAGNETOMETER DESIGN

The DSX magnetometer design is based on that used for ST5, and we describe the development effort for the ST5 magnetometer in some detail (see also UCLA's ST5 web-site http://www-ssc.igpp.ucla.edu/st5). UCLA's ST5 fluxgate magnetometer is the product of a long series of successful spaceflight magnetometers. The sensors are boom mounted and have no active components. Drive, sense and feedback signals travel along the boom cable between the sensors and the electronics board on the spacecraft. The electronics whose functional block diagram is shown in Figure 5 generates the fluxgate

drive signal, detects the second harmonic of this signal, nulls the field surrounding the sensor, and provides a digital reading of the current needed to null each of the sensors. This signal is then sent to the telemetry system. There is no microprocessor in this simple design.
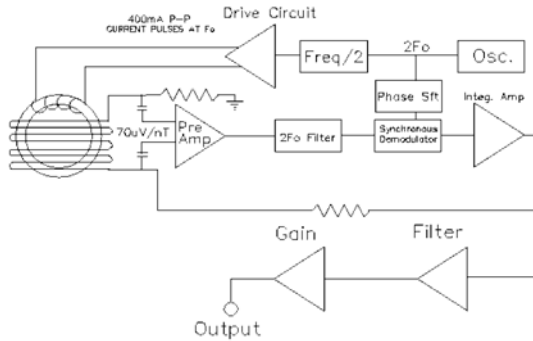
Figure 5. The functional block diagram of the UCLA ST5 fluxgate magnetometer showing its drive, sense and feedback circuits.

2.4.1 Fluxgate Sensors

A fluxgate magnetometer is the best choice for the DSX objectives because of its extensive heritage on space missions and superiority to other magnetometer types. By way of comparison, we have examined other devices in our laboratory such as the new Hall Probe chips and the gross magnetoresistive resistor (GMR) magnetometers. These devices have little or no flight history, and have noise and offset stability performances that are several orders of magnitude higher than that required for either the DSX or ST5 projects.

The fluxgate sensors in the UCLA magnetometer are manufactured using the latest low-noise ring-core technology. The ring bobbin is machined from Inconel X-750. The magnetic material wound on the bobbins is low-noise 1/2-mil-thick 6-81.3 Mo-Permalloy. This material was first developed at Naval Ordnance Laboratory, White Oak, in 1968, by *Gordon, Lundsten, Chiarodo and Helms* [1968].

UCLA purchased the last of the ring-core material in 1998 and had it fabricated into small (3/8" and 5/8") cores in anticipation of future missions. The sensors are similar to our standard design flown on many previous missions. The feedback windings enclose the cores so that in operation the cores themselves are never exposed to strong fields orthogonal to the sense axis that can cause distortions at the level of about 1 part in 10^4 [*Brauer et al.*, 1997], as found on Magsat [*Acuna*, 1982]. The lack of active components on the sensors means that they are very tolerant of temperature extremes. They were qualified at over 100C on Galileo and have operated after being immersed in liquid nitrogen (-196C). The sensors require no heaters. Because UCLA fabricates its own sensors, it has complete quality assurance control of the assembly process, leading to

8

greater mission assurance. Figure 6 shows the sensor being fabricated for ST5. Because DSX is less mass constrained than ST5, we propose to use the same basic design with larger 1-inch cores. This increase in the mass of the sensor will result in lower noise levels.

Figure 6. The 3-axis ring-core fluxgate sensor fabricated by UCLA for ST5. A similar design is used for DSX. The DSX sensor occupies a volume of 5x5x5 cm.

2.4.2 Drive and Sense Circuits

The ST5 magnetometer uses the classic fluxgate circuit presented in Figure 7. Sensor mass and power are kept low with a dual-core series drive circuit. Thus, there is only one drive circuit needed for ST5. This single-drive circuit was used successfully on FedSat.

As part of our development effort for ST5 we have conducted noise and non-linearity tests for the fluxgate circuits. Noise levels are shown in Figure 8, and results from the non-linearity test are shown in Figure 9. Results for the DSX sensor were presented in previous Annual Reports.
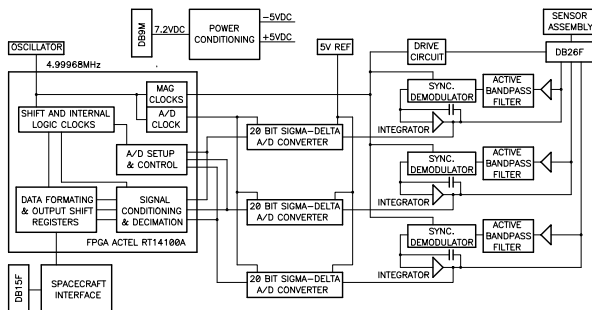
Figure 7. Basic fluxgate magnetometer circuit that has been used successfully in space by UCLA for 35 years. One of the keys to the excellent linearity, stability and noise of the UCLA implementation of this circuit is careful selection of parts.

9
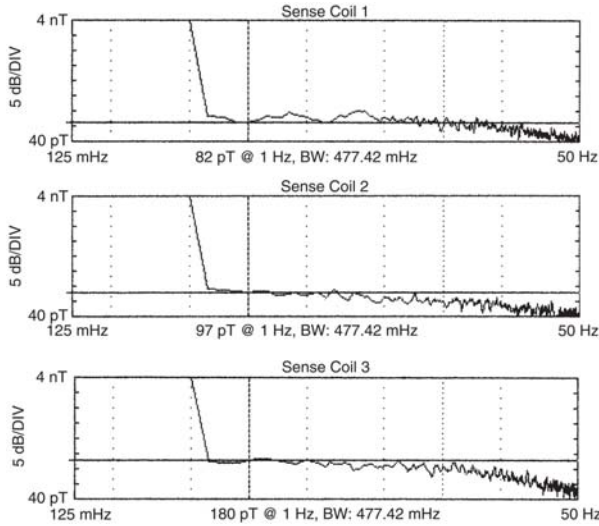
Figure 8. Noise level tests for the ST5 magnetometer.

From Figure 8 we see that the noise levels are of order 100 pT RMS at 1 Hz, with a 500 mHz bandwidth. These noise levels are clearly adequate for the DSX mission requirements. Moreover, the measured non-linearities are well within DSX requirements.
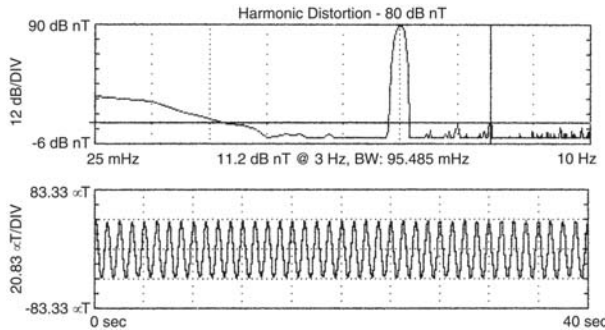
Figure 9. Non-linearity tests for the ST5 magnetometer. The magnetometer is excited with a 1-Hz tone. Harmonic distortion is below –80 dB.

2.4.3 Analog to Digital Converter

The specifications for the ST5 magnetometer called for 17-bit conversion of the measured fields. The AD7714 sigma-delta converter was selected and has been qualified for ST5. ST5 launched in 2006.

Within the ST5 magnetometer, the magnetic field is sampled at 96 vectors/second. The data are then recursively filtered to provide data at 16 vectors/second to the spacecraft telemetry. This digital filtering has been a standard feature of UCLA magnetometers, as it reduces aliasing by signals above the Nyquist frequency, and also improves the noise characteristics of the magnetometer. For DSX we propose to provide a data rate of ~ 20 Hz.

2.4.4 ST5 Magnetometer Properties

The properties of the ST5 fluxgate magnetometer are summarized in Table 2. These are included here as the baseline from which we will derive the specifications of the DSX fluxgate magnetometer.

Table 2. Summary of ST5 Magnetometer Properties.

ST5 Mechanical Properties	
Sensor Mass	75 g
Sensor Volume	4x4x6 cm
Electronics Mass	250 g
Chassis Mass	250 g
Chassis Volume	10x12x8 cm
Interface Cable	66 g
ST5 Electrical Properties	
Sensor Power	50 mW
Electronics Power	500 mW
ST5 Characteristics	
Dynamic Range	+/- 64,000 nT
Resolution	1 in 64,000 nT
	0.1 in 1000 nT
Sample Rate	16 vectors/s
Absolute Accuracy	< +/- 0.01%
Noise (0.5 Hz bandwidth)	< 0.1 nT rms
Orthogonality Knowledge	< 0.1 deg
Alignment Knowledge	< 0.1 deg

2.5 DSX VMAG DESIGN

The following discussion summarizes the design of the DSX VMAG. Material was drawn from Data Package prepared by UCLA for the PDR and CDR and previous reports.

2.5.1 Mechanical Design

The VMAG fluxgate derives heritage from a long line of UCLA magnetometers. The design is a more rad-hard flow down from the NASA ST-5/Polar magnetometer. The sensor is shown in Figure 10 and the electronics board in Figure 11. The printed circuit board (PCB) is housed in aluminum and hard mounted to the spacecraft. The VMAG Flight electronics board was completed in 1Q 2008 and is shown in Figure 12. The physical properties of the VMAG instrument is shown in Table 3.

The Flight Unit Electronic Unit Chassis and Sensor Chassis were completed during the 4Q of 2007 and they were nickel plated during the 1st quarter of 2008. During the 2Q, the flight units were painted and labels were ink stamped onto the chassis.

Table 3. VMAG Physical Properties.

VMAG Mechanical Properties	(g or cm)
Sensor Mass	500
Sensor Volume	11.1x6x8
Electronics Mass	240
Chassis Mass	1360
Chassis Volume	24x14x3.2
Interface Cable	160 g/m
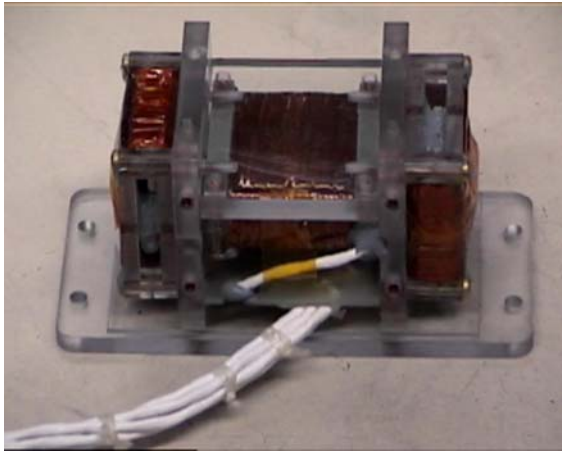
Figure 10. Sensor: 6.0 x 11.1 x 8.1 cm.

Figure 11. Development Unit: 11.4x20.32 cm.

Fabrication of the flight sensor was completed in the 3Q 2008. The flight sensor was integrated with the flight EU for testing at the end of the quarter and was part of the functional and thermal testing. Completion of the sensor fabrication ("buttoning it down") as well as completion of the final flight cable 33" segment that connects the EU with the spacecraft bus for connection to the sensor cable and boom was also completed in 3Q 2008. Figure 13 shows a picture of the flight sensor next to the painted chassis and Figure 14 shows the flight sensor with the GSE Helmholtz Coil inside shield cans being tested.
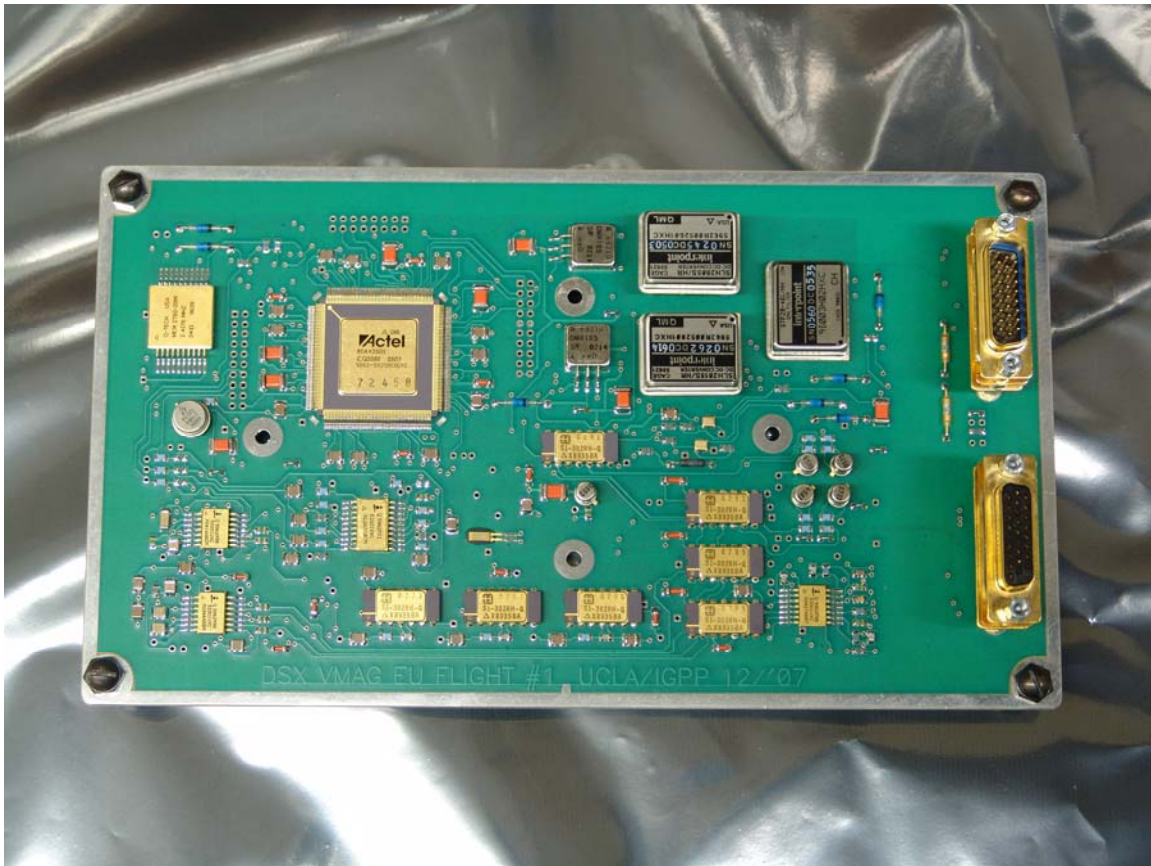
Figure 12. VMAG Flight Electronics Board

Figure 13. The Flight sensor, chassis and a US quarter for scale.
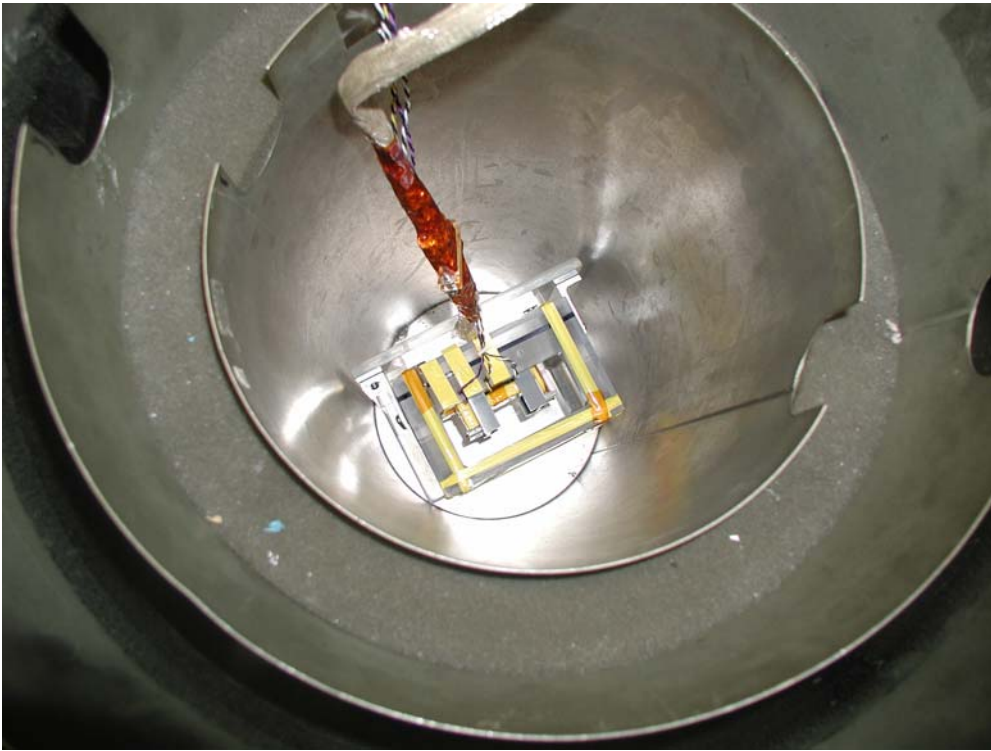
Figure 14. Looking down into the magnetic shield can at the flight sensor inside the GSE Helmholtz coil attached to a testing tip-plate.

Prior to the flight unit completion in 2008, the VMAG team supported two DSX meetings. One was DSX system CDR in Colorado in mid-May, in which Don Dearborn represented the team. The second meeting was a two-day site visit by Elsner, Sillence and Stuart at UCLA (May 20 & 21). The Site Visit gave the VMAG team the opportunity to meet Sillence and Stuart and to show the significant progress on the development of the engineering and flight units. We also demonstrated some of the I&T testing procedures.

The 2nd Ground Support Equipment (GSE) development was completed during 3Q 2008. The hardware included the control box and Helmholtz coil (Figure 15 is one test set up with the shield cans). Labview programming provides simple interfaces for some of the tests required (such as the BAT).

Figure 15. GSE control box (top of image), PC (middle), and shield cans (bottom). Figure 14 is looking down into the shield cans. Next to the PC and multi-meter on the bench is the engineering electronics unit.

2.5.2 VMAG Mechanical Fabrication

The Mechanical Fabrication Approach was the following.

- All in-house procedures and tests involving flight instrument performed by NASA certified technicians.

- Incoming flight parts were inspected, kitted and stored.

- PCB manufactured by outside contractor (Cirtech), to MIL-PRF-55110.

- PCB coupons tested and certified by independent contractor (DELSEN Labs).

- EU chassis milled to specification at Bellfx LLC

- Sensor chassis milled to specification / drawing in-house.

- PWA assembled using AIDS.

- EU and sensor chassis tested for fit, plated by outside contractor (California Technical Plating) to UCLA0280-PLT.doc, and painted in-house to UCLA0240-PNT.doc.

- Sensor and EU chassis inspected in-house.

- Sensor ring cores wound in house.

- Sensor Bobbins and armature parts machined to specification/drawing.

- Sensor ring cores, bobbins, armature parts and EU PWA inspected in-house

- Sensor assembled (except for cover) and pigtail cable attached to sensor.

- Sensor assembly inspected in-house.

- Flight and engineering model boom cables constructed by UCLA

- Flight boom cable inspected by UCLA personnel.

- After engineering test, tuning, and qualification, the PWA was inspected in-house.

- PWA conformal coated and given final QA inspection in-house.

- PWA installed in EU chassis and cover installed on sensor assembly.

- Instrument subject to environmental testing and burn-in.

- The structural models were developed using SolidWorks® and submitted to the DSX PMO.

2.5.3 Mechanical Interface

Drill templates were supplied for mounting the VMAG sensors and electronics unit to the spacecraft. The physical mounting location of the VMAG sensor was determined by DSX and spacecraft contractors. The VMAG sensor is boom-mounted to reduce the effects of spacecraft-induced-magnetic fields.

The sense axes of the fluxgate magnetometer do not physically align exactly with the axes of the sensor assembly. As part of the VMAG calibration, sense-axis alignment were determined to within 0.01 degrees accuracy with respect to reference axes of the VMAG sensor assembly. See ICD for more details.

2.5.4 Electrical Design

The basic electrical design is described in the heritage section of this report. Details of the VMAG electrical design can be found in the CDR package and the electrical properties are give in Table 4.

Electrical power is to be supplied to VMAG at 28 VDC. VMAG includes power conversion and conditioning circuits, as well as ripple and transient protection. On-orbit experience with FAST indicates that no survival heaters are required, although thermal regulation is included for normal operations. VMAG has one operation mode – ON.

Table 4. VMAG Electrical Properties

Sensor Power	50 mW
Electronics Power	1.95 W

2.5.5 Ground Support Equipment

The GSE is the VMAG interface that performs the following:

- Supplies Power to VMAG EU.

- Converts RS-422 serial interface from VMAG EU into formatted USB data stream.

- Monitors VMAG EU temperature and current.

- Provides access to internal VMAG test interface.

- Provides stimulus current for shield can coils and Helmholtz coil.

- Provides support for SFT, BAT and thermal vacuum/thermal cycle tests.

Deliverables included the following:

- Laptop Computer (Dell Latitude D510)

- GSE chassis

- 26 conductor cables between GSE chassis and VMAG EU (with connector savers)

- USB cable between GSE chassis and laptop.

- GSE manual

- Helmholtz coil

- Magnetic shield can (on loan to project)

- 3 BNC

- Breakout box

The GSE uses LabView® and is Ethernet capable for remote operation. Figure 16 shows the LabView® interface and Figure 17 shows the front panel of the GSE.

Figure 16. Display of VMAG GSE.

Figure 17. Picture of GSE Chassis.

On the basis of prior flight heritage, the VMAG parts and sub-assemblies will survive the Mid-Earth orbit environment for the duration of the DSX spacecraft lifetime.

The appropriate coatings and finishes, based on MIL-STD-1547, will be used for VMAG.

2.5.6 Electrical Interface

The Electrical Interface is described in the ICD. A summary of the interface is as follows:

- EU has two connectors. One for spacecraft interfaces (ECS and HSB). One for VMAG Sensor.

- Power (HSB I/F) and Signal (ECS I/F) share a single connector: 26 Contact Hi-Density D-Type Male. Manufacturer: Positronics Industries, Inc., Part #: SDD26M3P0T2.

- Sensor: 26 Contact Hi-Density D-Type
Female. Manufacturer: Positronics Industries, Inc., Part #: SDD26F3P0T2.

2.5.7 Thermal Interface

The thermal design for VMAG does not use the spacecraft as a heat source or sink. Any heat transfer will be via the electronics unit baseplate, although some conduction via cabling cannot be avoided. The power dissipated by the VMAG electronics unit (EU) is 2.5W, well below the 10 W limit for conducted heat transfer.

VMAG is designed to operate within specifications over the range –10º C to +40º C. VMAG is also designed to survive in the range –40º C to +50º C.

Details can be found in the Thermal Analysis Memo of the CDR data package.

2.5.8 Materials List

VMAG does not have any Hard Magnetic Material.

Table 5. Metallic Materials List

All in accordance with CRD 4-9.1, and 4-9.2
Aluminum, 6061-T6 (Structure)
Electroless Nickel Plate (Finish on Chassis)
Copper (Tape)
Silver coated Copper (Braid, Bus wire)
Brass (Fasteners)
Brass, silver plated (Bifurcated terminals, Turret terminals)
Phosphor Bronze (Springs, Helicoils)
Solder 63/37
Inconel X750 (Sensor Ring)
Permalloy (Sensor Ring)
Kovar (EEE Parts)

Soft Magnetic Material List
Permalloy-Sensor Ring
Kovar-EEE Parts

2.5.9 Parts

The VMAG contains no pressurized systems.

All parts, materials, and processes are in accordance with MIL-STD-1543B requirements.

No toxic outgassing occurs as part of VMAG design and construction.

Parts were selected from GSFC PPL, NPSL, MIL-STD-975, or the DSX contractor's Parts Management Plan.

Class I Ozone Depleting Substances (ODS) are not used. Class II ODS and other substances requiring public notification under Federal and State laws shall be eliminated wherever possible.

UCLA has a full Hazardous Materials Program.

Table 6. Electronics Parts List

Parts procurement from GSFC PPL-21 wherever possible.
Resistors – MIL-R-55342 & MIL-R-39007
Capacitors – MIL-C-55681, MIL-C-123, and MIL-C-55365
Fuses – MIL-F-23419
Connectors – MIL-C-24308, GSFC-S-311-P-4
Diodes & transistors – MIL-S-19500
Microcircuits – MIL-M-38535, Rad level R or better
RH1021-BMH-7 (internal spec equivalent to 38535)
Hybrid- spec MIL-PRF-38534
Crystal Oscillator (internal spec equivalent to 38534)
Thermistor – GSFC-S-311-P-18
Cable- NEMA-W-2500

2.5.10 Flight and Test Software Design

The VMAG is a "state machine" that has no programmable components when on-orbit. The command interface is kept as simple as possible to provide for robust and reliable operations. GSE for the VMAG is PC-based, and includes Ethernet connectivity for interfacing with the spacecraft electrical GSE. The telemetry is handled by the ECS.

2.5.11 Integration and Test

All calibration was done at UCLA using UCLA equipment. The following tests were conducted pre-launch:

Noise Test
Overnight test in quiet environment (flux can, quiet site) (Fig. 8).
Linearity Test
Apply oscillating magnetic field; search for harmonic signal. (Fig 9)
Zero Level Test

Reverse sensor directions in low field (flux can).
Repeat as a function of temperature.
<u>Scale Factor Test</u>
Apply known magnetic field; measure output.
Repeat with varying temperature.
<u>Orthogonality Test</u>
Apply fields along axes of magnetometer; sense orthogonal readings.
<u>Frequency Response Test</u>
Apply oscillating signal of varying frequency; measure amplitude and phase of output.

2.5.12 Documentation

VMAG was documented to the specifications of the DSX Program Office in the following documents:
- ICD (Interface Control Document)
- PSRD (Performances Specification and Requirements Document) folded into ICD
- RVM (Requirement Verification Matrix)
- QAP (Quality Assurance Plan)

A detailed UCLA Document Tree describing all internal UCLA documentation is included in the CDR package.

2.5.13 Analysis

UCLA has a quality assurance plan that is consistent with ISO 9001. Appropriate controls and record keeping were used throughout the fabrication and testing processes. Such controls and record keeping apply to tools, facilities, and sensor units. GSE has inspection and test records.

During unit fabrication, all sub-assemblies were tested for compliance with requirements, and visually inspected for defects. Unacceptable parts were rejected. Unacceptable sub-assemblies are reworked and retested.

All changes to designs were tested for conformity to performance specifications and reported to the PMO.

2.5.14 The UCLA Team

The project team for the UCLA VMAG project is shown in Table 7. No change in personnel occurred from previous years.

Table 7. UCLA VMAG Project Team and Basic Responsibilities

Name	Role and Responsibilities
Dr. Mark Moldwin	<u>PI</u>, overall project oversight, interface to DSX PMO, coordination of efforts of various project members, science lead
Dr. Robert Strangeway	<u>Science Team</u>

Mr. Joe Means	Project Manager, Schedule, budget manager
Mr. Dave Pierce	Electrical Engineer Design
Ms. Kathryn Rowe	Systems Engineer Design and Testing
Mr. Don Dearborn	Digital Engineer Programming and Testing
Mr. William Greer	Electronic and Mechanical Technician Fabrication and Testing
Mr. Bob Snare	Q&A testing, magnetic cleanliness

3. YEAR IN REVIEW

This section describes in detail the activities of the Final Year of the project. At the end of each quarters description is the level of effort and personnel that were involved in DSX VMAG activities for that quarter. Though Moldwin participated in regular telecons, engineering meetings and wrote the quarterly and annual reports for the project, he was directly supported under DSX for only one-month during the 3Q (summer) while at UCLA.

3.1 Summary of Activities 2Q 2009

The main activities of the quarter were participation in I&T preparation activities and WPIx discussions. Hardware was delivered 4Q of 2008. UCLA shipped the VMAG Engineering Unit with a current source to Sierra Nevada Corporation (SNC) on April 10, 2009 and supported the IAS-ECS/VMAG EU test the following week (April 13). The test was successful.

The PMO requested our input and approval for the depressurization rates, which were reviewed and approved on April 14, 2009. The PMO also distributed for approval the Z Antenna ICD Rev B. The document was reviewed, some minor comments submitted (noting that the tip plate had been slightly modified in response to a fit check done with the VMAG Sensor at ATK last year) and approved. The PMO requested information about the commissioning sequence. VMAG is a very simple instrument with the only command needed is "power on". Ideally we would be powered on during boom deployment in order to measure the spacecraft fields.

During the quarter, Kathryn Rowe and Dave Pierce also developed the Helmholtz feedback methodology to support DSX I&T (using Octant CGS). A Memo describing theI&T options was provided to the PMO on May 14, 2009.

The PI (Mark Moldwin) moved from UCLA to the University of Michigan at the end of June and was moving or on international travel for much of the quarter. Joe Means was the VMAG team member contributing to VMAG discussions on WPIx. However, Prof. Moldwin remains an adjunct professor at UCLA and continues to lead the DSX VMAG efforts.

3.2 Summary of Activities 3Q 2009

The main activities of the quarter was participating in discussions and planning for integration and testing. This included developing Safe-to-Mate procedures, providing magnetic cleanliness support, and the discussion of CONOPS.

Based on preliminary calculations, VMAG electronics would be exposed to very large fields during high power transmission in the VLF frequency range. However, subsequent analysis demonstrated that the simplified electromagnetic field environment model was flawed, and the fields that VMAG will be exposed are much smaller. The development of a testing procedure was done this quarter. The VMAG team also asked for a more detailed analysis of the expected magnetic field, as the estimates where much higher than expected.

Mark Moldwin re-joined WPIx discussions after the move in August along with Joe Means. One of the primary activities of the quarter was the participation at the 15-18 September 2009 Lake Arrowhead DSX Science meeting. Bob Strangeway and Mark Moldwin participated. We had fruitful discussions with Steve Stelmash regarding potential interference of VMAG by the VLF transmitter during High Power Transmissions.

Moldwin: 3Q09 30% Means: 3Q09   10%; Rowe: 3Q09   5%; Snare: 3Q09   3%; Uy: 3Q09   10%

3.3   Summary of Activities 4Q 2009

The main activities of the quarter were participation in I&T preparation activities and WPIx discussions. Due to travel of key personnel and DSX PMO testing activity, there was no VMAG activity in October.

Based on preliminary calculations, VMAG electronics would be exposed to very large fields during high power transmission in the VLF frequency range. The development of a testing procedure was done 3Q 2009 quarter. The VMAG team also asked for a more detailed analysis of the expected magnetic field, as the estimates were much higher than expected. The re-analysis by Lincoln Lab showed that the magnetic field strength at the VMAG electronics unit is much more reasonable and within expectations (100 nT instead of 100,000 nT). A white paper summarizing the environment predictions included UCLA results. Preliminary testing from 100 Hz – 30.8 KHz range, shows that VMAG is not saturated. The VMAG will operate properly up to +/- 100 Hz of the $2f_o$ frequency (~30KHz) as long as the field amplitude is less than 1000nT. When the frequency approaches the $2f_o$ point the magnetometer will start to see affects as the fields interact with our circuits. This effect will be evident no matter what fields are produced by the transmitter.

The relevant section of the White Paper that was submitted to the PMO describing the analysis is reproduced here.

Magnetic Field

The magnetic field was simulated at both ends of the z-boom, one containing TASC and the other end the VMAG. By symmetry, the magnetic fields at the ends should be about the same with z and x components dominant, and the simulations bear this out. The two H-field plots use the same simulation with the marker frequency simply moved to provide values at two frequencies of interest. The simulation was numerically

stable and produce results that are illustrative of the dispersive media affect on the field values and the results are shown in Figure 18. Below cutoff, the magnetic field is approximately the value expected in the electrostatic limit, which was calculated to be approximately 125 nT given a line current of 5 amps and distance of 8 meters from the y-boom axis to the z-boom tip, which favorably compares with the 73 nT and 79 nT in the simulations. Above cutoff, the displacement term of Ampere's Law adds to the magnetic field. No symmetry planes were enforced in the simulation, which leads to longer computations but it removed a somewhat artificial bound since the spacecraft isn't perfectly symmetrical across any of the principal planes due to the positioning of payloads.
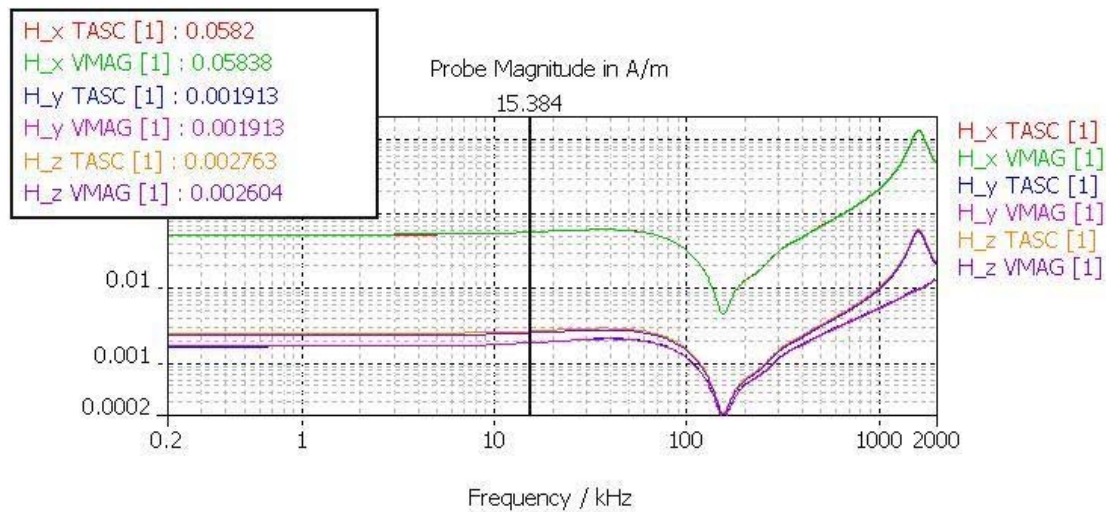

Figure 18: H-fields at the tips of the z-boom, TASC and VMAG locations, with marker at 15.4 kHz. Applied y-boom dipole voltage amplitude is 5 kV and the surrounding medium is an isotropic electron plasma with a plasma frequency of 159 kHz. A significant change in the fields is noted at the y-boom dipole resonant frequency of 1,680 kHz. The peak value of 0.0582 A/m at 15.4 kHz is equal to 73 nT.

The planning for a more detailed sweep frequency test of VMAG was scheduled for January 10, 2010. A December 8, 2009 telecon with the PMO was conducted to discuss the procedure. The telecon discussed the next test of the VMAG EM (in January). The objective of the test was to determine the maximum angular error that the TNT-induced field will impose on VMAG and how long it will take to recover over the TNT operating frequency range of 1 kHz – 50 kHz for high-power VLF Tx. The requirement on the ADCS is 1 degree threshold with a 0.1 degree objective. The VMAG team developed a test plan to verify and measure the transient response. Integration planning ramped up considerably as I&T was scheduled for the February/March 2010 timeframe. The main issue was controlling the Helmholtz Coil without VMAG GSE during DSX AI&T.

Discussions with the PMO and contracting officer continued regarding follow on support for I&T as the Period of Performance (PoP) ends in March 2010.

Rowe: 4Q09   5%; Snare: 4Q09   3%; Uy: 4Q09   3%

3.4 Summary of Activities 1Q 2010

The first quarter of 2010 included significant work to resolve the High Power transmission issue and the development of the GSE and Helmholtz system for I&T.

The main issue with the high power transmission was that VMAG is susceptible to power at our $2f_o$ frequency and will provide unreliable data to the spacecraft during those times. A test was conducted to determine the magnitude of the problem and the time it would require to recover any transients. Figure 19 shows the results of the sweep frequency test on the EU VMAG. A 100 nT Peak-to-Peak (P-P) signal was applied near the $2f_o$ and the P-P amplitude of the resulting tone was measured. The tone observed in VMAG was measured, recorded and plotted. The frequency of the observed tone corresponds to the difference frequency between the applied tone and $2f_o$. Signals outside of the band 30.68 kHz to 30.76 kHz will not affect the operation of VMAG. Signals inside this band will introduce tones in VMAG with signals exactly at $2f_o$ causing DC shifts. There is a little attenuation of the signals in the Aluminum housing observed (100 nT applied signal results in 80 nT observed signal). The sensor returned to normal operation within 300 msec.
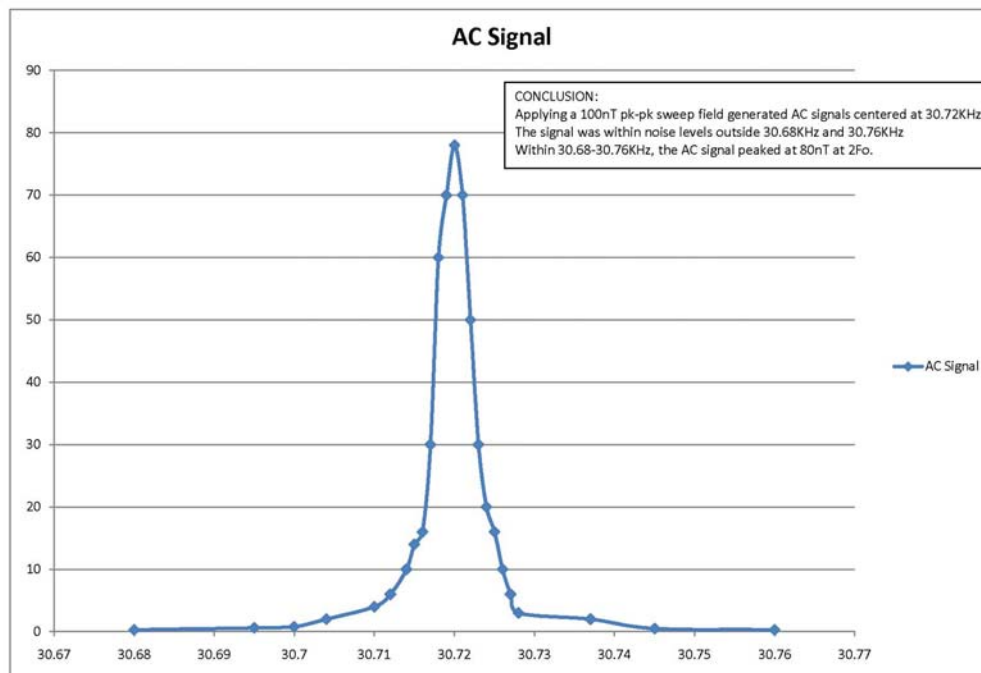
Figure 19. The results from sweep frequency test.

To help address this issue, a transmitter frequency restriction (30.5-31.5 kHz) has been implemented via the TNT Restricted Frequency List by UML. (It's in the latest FSW release and has already been tested).

The VMAG GSE was modified in accordance with our recommended approach and the packet definition was sent to the DSX I&T team. After some delay, the I&T team was ready to support the UCLA onsite visit (Dave Pierce) for GSE software installation, test & verification the week of 29 March. David Pierce successfully installed the new Helmholtz coil control software on the VMAG GSE on March 29. There were a few wrinkles that had to be worked out (sending/receiving packets, etc.) but the effort was a success. No major issues with the physical mounting of the VMAG on the Z-boom later in April were anticipated.

Means: 1Q10   10%; Rowe: 1Q10   5%; Uy: 1Q10   11%

4. CONCLUSIONS

The UCLA VMAG team delivered the VMAG flight hardware in the 4Q of calendar 2008. The testing of the DSX vector magnetometer indicates that the magnetometer will perform better than the requirements and will contribute significantly

to the science objectives of the mission. Last year we attended the first DSX Science meeting, and began the Integration and Testing of VMAG with the spacecraft.

This effort has demonstrated that the new sigma-delta magnetometer design, that is a direct follow-on to the successful NASA ST-5 magnetometer, can provide a research grade system in a low-mass and power package. The movement of more of the analog circuitry into the digital domain, also allows the design of more radiation tolerant designs. The DSX VMAG science team looks forward to a successful launch and the analysis of the radiation belt science data from the mission. With the current timing of the launch, the DSX mission should benefit from and directly contribute to greater understanding of the radiation belts by making simultaneous measurements with NASA's Radiation Belt Storm Probes (RBSP) , the Canadian Orbitals mission and the Japanese ERG mission.

REFERENCES

Acuna, M. H., The UOSAT magnetometer experiment,, Radio and Electronic Engineer, vol. 52, Aug.-Sept. 1982, p. 431-436.

Anderson, B. J., M. J. Engebretson, S. P. Rounds, L. J. Zanetti, and T. A. Potemra (1990), A Statistical Study of Pc 3-5 Pulsations Observed by the AMPTE/CCE Magnetic Fields Experiment, 1. Occurrence Distributions, *J. Geophys. Res.*, 95(A7), 10,495–10,523, doi:10.1029/JA095iA07p10495.

Baker, D. N., J. B. Blake, L. B. Callis, J. R. Cummings, D. Hovestadt, S. Kanekal, B. Klecker, R. A. Mewaldt, and R. D. Zwickl (1994), Relativistic electron acceleration and decay time scales in the inner and outer radiation belts: SAMPEX, *Geophys. Res. Lett.*, 21(6), 409–412, doi:10.1029/93GL03532.

Bortnik, J., U. S. Inan, and T. F. Bell (2003), Energy distribution and lifetime of magnetospherically reflecting whistlers in the plasmasphere, *J. Geophys. Res.*, 108(A5), 1199, doi:10.1029/2002JA009316.

Brauer, J.R.; Lee, S.H.; Chen, Q.M.; , "Adaptive time-stepping in nonlinear transient electromagnetic finite element analysis," *Magnetics, IEEE Transactions on* , vol.33, no.2, pp.1784-1787, Mar 1997, doi: 10.1109/20.582621

Gordon, D.; Lundsten, R.; Chiarodo, R.; Helms, H., A fluxgate sensor of high stability for low field magnetometry, IEEE Transactions on Magnetics, vol. 4, issue 3, pp. 397-401, 1968.

Le, G. and C. T. Russell, Effect of sudden solar wind dynamic pressure changes at subauroral latitudes: Time rate of change of magnetic field, *Geophys. Res. Lett., 20,* 1-4, 1993.

Li, X., D. N. Baker, T. P. O'Brien, L. Xie, and Q. G. Zong (2006), Correlation between the inner edge of outer radiation belt electrons and the innermost plasmapause location, Geophys. Res. Lett., 33, L14107, doi:10.1029/2006GL026294.

Moldwin, M. B., L. Downward, H. K. Rassoul, R. Amin[1], R. R. Anderson, A New Model of the Location of the Plasmapause: CRRES Results, *J. Geophys. Res., 107* (A11), 1339,
  doi:10.102912001JA009211, 2002.

O'Brien, T. P., K. R. Lorentzen, I. R. Mann, N. P. Meredith, J. B. Blake, J. F. Fennell, M. D. Looper, D. K. Milling, and R. R. Anderson, Energization of relativistic electrons in the presence of ULF power and MeV microbursts: Evidence for dual ULF and VLF acceleration, *J. Geophys. Res.*, 108(A8), 1329,
  doi:10.1029/2002JA009784, 2003.

Ozeke, L. G., and I. R. Mann (2008), Energization of radiation belt electrons by ring current ion driven ULF waves, J. Geophys. Res., 113, A02201, doi:10.1029/2007JA012468.

Tsyganenko, N.A., H. J. Singer, and J. C Kasper, Storm-time distortion of the inner magnetosphere: How severe can it get? *J. Geophys. Res., 108*, SMP 18-1, CiteID 1209, DOI 10.1029/2002JA009808, 2003.

(page left intentionally blank)

List of Symbols, Abbreviations, and Acronyms

A/D	analog to digital
ADC	analog to digital converter
ADCS	Attitude Control System
AE	Auroral Electrojet index
AFRL	Air Force Research Lab
AIDS	Assembly Instruction Data Sheet
AMPTE	Active Magnetospheric Particle Tracer Explorer
Asym	Asymmetric Ring Current index
ATK	Aliant Techsystems Inc.
ATS	Applications Technology Satellite
BAT	Bench Acceptance Test
BNC	Bayonet Neill-Concelman Connector
CCE	Charge Composition Explorer
CDR	Critical Design Review
CGS	Common Ground System
CONOPS	CONcept of OPerationS
CVCM	Collected Volatile Condensable Material
CY	Calender Year
DC	Direct Current
DOC	Department of Commerce
DOD	Department of Defense
DSRD	Draft Sensor Requirements Document
Dst	Disturbed Stormtime index
DSX	Demonstration and Science Experiments
ECS	Experiment Computer System
EDR	Environemental Data Record
EDU	Engineering Development Unit
EEU	Engineering Electronics Unit
EM	Engineering Module
EMC	Electromagnetic Compatability
EMI	Electromagnetic Interference
ERG	Energization and Radiation in Geospace
EU	Engineering Unit
FAC	Field-Aligned Current
FAST	Fast Auroral Snapshot Explorer
FedSat	Federation Satellite (Australia)
FPGA	Field Programmable Gate Array
f_o	VMAG Drive Frequency
FU	Flight Unit
FY	Fiscal Year
GEO	Geosynchronous Orbit
GEOS 2	Geosynchronous Orbit Scientific Satellite 2
GMR	Gross Magnetoresistive Resistor
GPS	Global Positioning System

GSE	Ground Support Equipment
GSFC	Goddard Space Flight Center
HEO	High Earth Orbit
HSB	Host Spacecraft Bus
I&T	Integration and Test
IAS	Integrated Avionics System
ICD	Interface Control Document
IGPP	Institute of Geophysics and Planetary Physics
IMF	Interplanetary Magnetic Field
IPO	Integrated Program Office
ISEE	International Sun-Earth Explorer
ISO	International Standardization Organization
ITAR	International Traffic in Arms Regulations
JPL	Jet Propulsion Laboratory
Kp	Planetary K index
LANL	Los Alamos National Laboratory
LCI	Loss Cone Imager
LEO	Low Earth Orbit
LSB	Least Significant Bit
LT	Local Time
McMac	Mid-Continent Magnetoseismic Chain
MEASURE	Magnetometers Along the Eastern Atlantic Seaboard for Undergraduate Research and Education
MEO	Medium-Earth Orbit
MSI	Microsat Systems Inc.
NASA	National Aeronautics and Space Administration
NOAA	National Oceanic and Atmospheric Administration
NPSL	NASA Parts Selection List
ODS	Ozone Depleting Substances
OGO	Orbiting Geophysical Observatory
PC	Personal Computer
PCAD	Personal Computer Aided Design
PCB	Printed Circuit Board
PDE	Principal Design Engineer
PDR	Preliminary Design Review
PET	Principal Electronic Technician
PF	Protoflight
PI	Principal Investigator
PMO	Project Management Office
PPL	Preferred Parts List
PSRD	Performances Specification and Requirements Document
PVO	Pioneer Venus Orbiter
PWA	Printed Wire Assembly
QA	Quality Assurance
RDR	Raw Data Records
RF	Radio Frequency
RMS	Root mean square
SACI-1	Satélite de Aplicações Cientificas
SAMBA	South American Meridional B-field Array

SAMPEX	Solar Anomalous and Magnetospheric Particle Explorer
SCATHA	Spacecraft charging at high altitude
SDE	Senior Development Engineer
SFT	Simple Functional Test
SMALL	Sino Magnetic Array at Low Latitudes
SNC	Sierra Neveda Corporation
SRD	Sensor Requirements Document
ST5	Space Technology 5
SymH	Symmetric ring current index
SWx	Space Weather Experiment
TASC	Tri-Axial Search Coil
TID	Total Integrated Dose
TBS	To be Specified
TML	Total Mass Loss
TNT	Transmitter and Narrowband Receiver
Tx	Transmitter experiment
UCLA	University of California Los Angeles
UCOP	University of California Office of the President
ULF	Ultralow Frequency Wave
UML	University of Massachusetts - Lowell
VDC	Volts Direct Current
VLF	Very Low Frequency
VMAG	Vector Magnetometer
WMM	World Magnetic Model
WPIx	Wave Particle Experiment